Surface Convective Heating Rates for a Double Swept-Wedge Configuration at Mach 6

R. Choudhury, J. Fuata, N. Stern and D. Buttsworth

Faculty of Surveying and Engineering
University of Southern Queensland, Queensland 4350, Australia

Abstract

A quantitative measurement of the global surface convective heating rates was achieved for a double swept-wedge model using a Mid Wave Infra Red (MWIR) camera. The configuration was tested in a free piston driven Ludwieg Tube facility producing test flows at a Mach number of 5.85 for about 200 milliseconds. The IR camera was calibrated based on a thermocouple instrumented copper plate heated up to the relevant surface temperatures. The calibrated IR images recorded at 100 frames per second were used to deduce the global surface temperature history of the model during the flow time. The temperature distribution is then converted to a heat flux distribution using an impulse response method. A flat plate model was also tested at nominally the same flow conditions and the data generated by the measurement technique was compared to an analytical model for a compressible laminar boundary layer heat transfer. A discrepancy of about 15% exists between the experimental and analytical data for the flat plate heat transfer calculations. Uncertainties in the substrate material properties are likely to contribute to this discrepancy.

Introduction

In the hypersonic flow regime (nominally Mach number 5 and above), the aerodynamic heating is a dominant factor because the convective surface heating rate varies directly with the cube of the velocity [1]. The high heat transfer rates presents challenges to the vehicle airframe. In particular, scramjet inlets are exposed to high localized heating. The principal mode of heat transfer during suborbital hypersonic flight is through forced convective heat flux. The heat transferred through the aerodynamic convective heating from the hot gas to the wall is given by:

$$\dot{q}_{convective} = h(T_r - T_w) \qquad (1)$$

where T_r is the recovery temperature and the T_w is the surface temperature and difference between them drives the convective heat flux and h is the convective heat transfer coefficient which is a function of the flow properties and can be expressed as:

$$h = C_H \rho_\infty c_p u_\infty \qquad (2)$$

where C_H is the Stanton number, ρ_∞ is the freestream density, c_p is the specific heat capacity and u_∞ is the freestream velocity.

Traditionally, experimental measurements of heat flux in high speed flow facilities with relatively low flow duration have been performed using fast-response thermocouples and thin-film heat-flux gauges. The thermal sensors measure the surface temperature rise during an experiment which is then converted to a heat flux value based on a semi-infinite solid assumption. Spatial variations in heat-transfer rates for complex geometric configurations can be hard to resolve using such discrete measurement techniques.

An Infra-Red (IR) camera can provide a global surface measurement technique. The advantages of this technique are that it does not require any external illumination sources, requires little or no surface treatment, is non-intrusive and can be highly accurate. Heat-transfer rates can be calculated from the surface temperature data and using appropriate data reduction techniques. Infrared thermography has been successfully used in plasma wind tunnels to measure surface temperatures of model re-entry vehicle surfaces [2] [3].

The double-swept wedge configuration is of interest because it models the cowl closure region of representative scramjet inlets, a region that is subjected to extremely high heat transfer rates. The Rectangular-to-Elliptical Shape Transition (REST) inlet is one such inlet [4]. The REST inlet is a promising scramjet inlet design that features a low-loss, mixed-compression inlet with a rectangular capture area that gradually morphs along the length of the inlet to yield an elliptical cross section at the combustor [5]. The cowl closure section in this configuration is susceptible to high heat-transfer rates. The high heating rates can be attributed to the complex interaction of the corner shock along with possible boundary separation/reattachment and development of vortical structures downstream.

Flow Facility and Model Instrumentation

The hypersonic facility used for the present experiments is the University of Southern Queensland's free-piston driven Ludweig tube designated "TUSQ". Further details of the facility and its operation have been described elsewhere [6]. The free piston driver quasi-isentropically compresses the gas between the piston and a 100 μm thick Mylar diaphragm placed at the entrance to the hypersonic nozzle. The test flow is initiated by the rupture of this diaphragm. The total duration of the steady flow is approximately 200 milliseconds. The test gas used during the present experiments was air. The total pressure and the total temperature produced during the experiments were 0.96 MPa and 550 K. A contoured nozzle with nominal Mach number of 6 and an exit diameter of 217.5 mm was used. Previous pitot pressure experiments show that the facility generates a inviscid core flow of about 160 mm diameter [7]. The flow unit Reynolds number is around $8 \times 10^6 \ m^{-1}$.
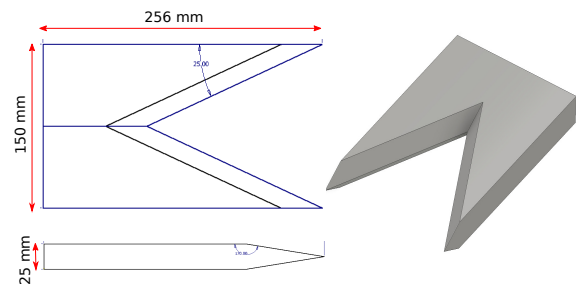

Figure 1: Double swept-wedge configuration used during the experiments.

A CAD model and the dimensions of the configuration used during the experiments are shown in Figure 1. The model was manufactured from Perspex (Polymethyl methacrylate). The measurement of heat transfer values using IR cameras in short-duration hypersonic facilities necessitates the use of materials with low thermal diffusivity such as Perspex. The low thermal diffusivity causes the amount of heat conduction through the model wall to be considerably lower than the heat load caused by the flow. This raises the surface temperature of the model and correspondingly yields a better signal strength for the IR camera.

The infra red measurements were achieved using a Xenics Onca Mid-Wave Infra Red (MWIR) camera. The Xenics IR camera has an Indium antimonide (InSb) array with 640×512 image resolution and outputs 14-bit images. The spectral bandwidth of the camera is 3.6 μm to 4.9 μm. The IR camera was mounted vertically with respect to the model as shown in Figure 2. A Calcium-Fluoride (CaF_2) window was used to be enable the transmission of the IR radiation at the mid-wave infra red spectrum. The transmission through the CaF_2 window for the 3-5 μm band is around 90%. An integration time of 5 milliseconds was used for the IR data acquisition at a frame rate of 100 Hz. The model was also instrumented with an Omega K-type (CO2-K) thermocouple. The thickness of the thermocouple is around 0.013 mm and it has has a response time in the order of milliseconds.
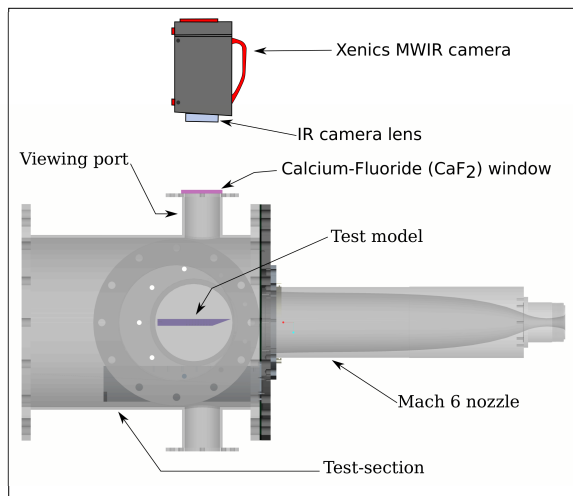

Figure 2: Xenics IR camera setup at TUSQ.

The current setup allows the IR camera to be adjusted both vertically and horizontally *w.r.t.* to the test model in the test-section. The IR camera lens allows the region of interest during the tests to be properly focused. The focus plane is currently set to be the mid plane of the Mach 6 nozzle parallel to the model support base. The current setup allows for a physical viewing area of roughly 100×80 mm.

IR Camera Calibration

The Xenics ONCA MWIR used during the experiments was used in its raw intensity mode. Hence, this required a calibration proccedure to be undertaken to be able to convert the intensity images generated by the IR camera to surface temperature distributions for the current configuration. The calibration of the IR camera was conducted using a $100 \times 80 \times 6$ mm thick copper plate heated by a hot plate. The copper plate was coated with a thin layer of Krylon KP-1602 Flat Black spray paint. This was done to increase the emissivity of the surface and provide a

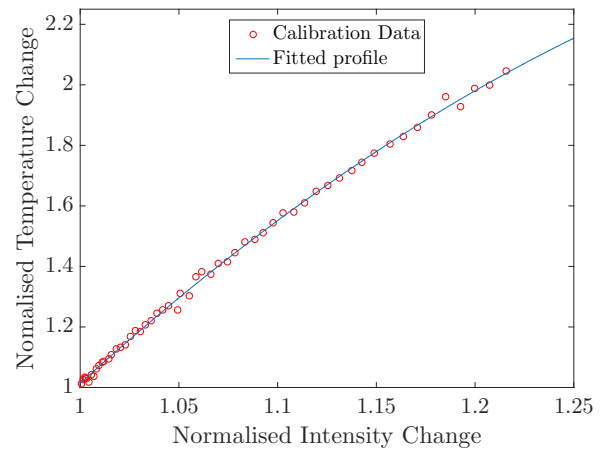better signal to noise ratio for the the IR camera.

Figure 3: Calibration of the IR camera using the heated copper plate.

The copper plate was instrumented with multiple surface thermocouples to monitor the uniformity of the surface temperature during the heat-up process. The high thermal conductivity of copper enabled a uniform surface distribution on the plate neglecting the edges. The intensity from a small averaged area of pixels from the IR camera in the vicinity of the thermocouple location was selected and compared to the corresponding temperature rise recorded by the thermocouple during the heating up process. The setup including the settings of the IR camera, distance of the IR camera relative to the configuration etc, were all matched to the experimental conditions during the actual flow run.

Figure 3 shows the calibration data acquired for the copper plate test and the second-order polynomial fit to the calibration curve. In Figure 3, the intensity change of the IR camera is normalised to the initial starting intensity at room temperature and compared to the temperature change recorded by the thermocouple during the calibration process normalised to the initial room temperature.

Experimental Results

The IR camera was used to record intensity change of the model surface radiation during the experiment. The model was also spray painted with high emissivity Krylon flat black paint to match the surface emissivity of the calibration experiments and increase the signal intensity of the infra red images. The images were recorded at a rate of 100 Hz during the flow experiments.

Figure 4 shows the comparison between the temperature measured by the surface thermocouple and the temperature rise measured by the IR camera at the corresponding thermocouple location based on the heated copper plate calibration during the test flow time. The data shown in Figure 4 has been shifted such that the flow starts at time $t = 0s$, and the end of the test time is at $t = 0.2s$. There is a good agreement between the surface temperature rise recorded by the thermocouple and the IR camera calibrated data using the heated copper plate technique.

Figure 5 shows the normalised IR intensity of the the model at the end of the 200 milliseconds of flow time. The leading edges of the model shows a higher intensity which is to be expected. The cowl closure section, where the two symmetrical sweeping sections merge is subjected to higher temperatures hence higher heat transfer levels due to corner shock and boundary layer interaction. Downstream of the corner region the IR images sug-
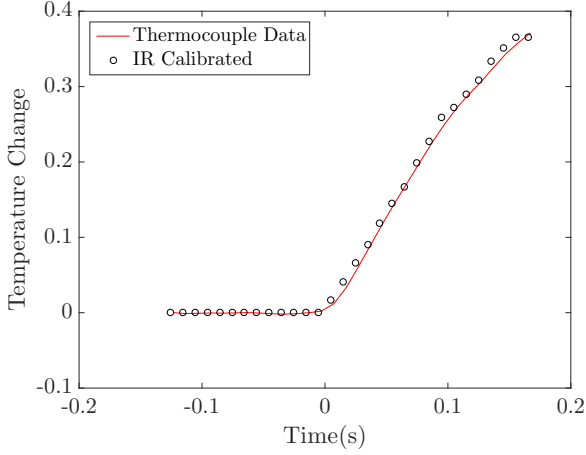
Figure 4: Comparison of the temperature rise recorded using a K-type thermocouple and the the calibrated IR camera temperature at the corresponding location.

gest the presence of symmetrical vortical structures.

The surface temperature distribution maps derived by using the IR camera calibration were then converted to heat flux maps using an impulse response method [8]. The calculated average convective heat flux distribution for the duration of the flow time is shown in Figure 6. The heat flux map follows a similar pattern to the IR camera intensity map. The surface thermocouple strands introduce some surface non uniformity and this leads to regions of small high heat flux areas on map. The non-uniformity in the surface heat flux distribution in Figure 6 is due to the complex natue of the flow described ealier as a result of the three dimensional nature of the model. A more detailed analysis is required to fully understand and characterize the flow field. The double-swept wedge was chosen as a test case to demonstrate the capability of this technique for a complex geometry with non-uniform flow features and heat-flux distribution.
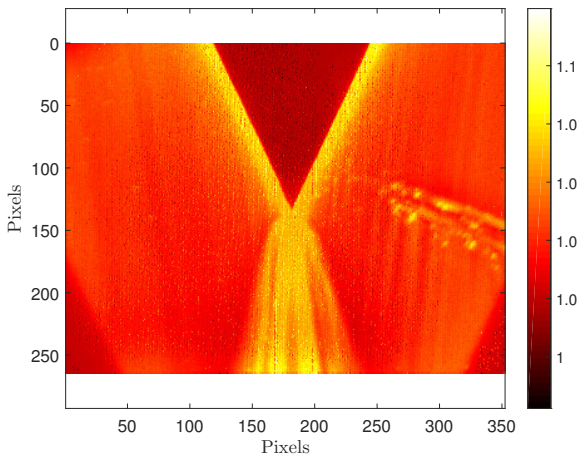

Figure 5: Normalised IR intensity map for the model at the end of the test flow. Flow direction, top to bottom.

For the purposes of verification of the experimental procedure and the comparison of the experimental data with analytical predictions, a separate experiment was conducted with a flat plate model. A similar procedure to that described for the double swept-wedge configuration was undertaken at the tunnel flow

conditions. The heat flux distributions on a flat plate derived from the IR camera were compared with compressible laminar boundary layer heat transfer calculations.
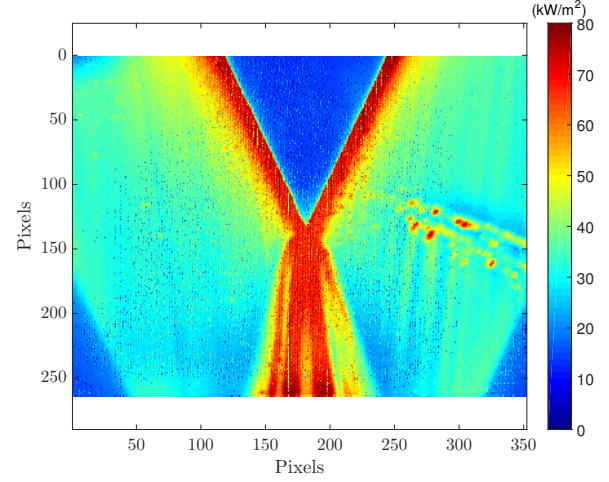

Figure 6: Average heat flux distribution for the model during the test time.

The analytical solutions are based on the reference temperature method [9]. In this method the the recovery temperature in Equation 1 is calculated such that:

$$T_r = T_e + r(V_e^2/2c_p) \qquad (3)$$

V_e is the velocity at the edge of the boundary layer and c_p is the specific heat capacity of air at constant pressure. The recovery factor, r in the above equation for a compressible laminar boundary layer is calculated using the equation:

$$r = \sqrt{Pr^*} \qquad (4)$$

The Prandtl number, Pr^* is introduced at a reference temperature described by the equation:

$$T^* = T_e + 0.5(T_w - T_e) + 0.22r[(\gamma - 1)/2]M^2 T_e \qquad (5)$$

here T_e is the temperature at the edge of the boundary layer, T_w is the wall temperature, γ is the ratio of specific heat for air and M is the Mach number. The local wall shearing stress τ_w and the friction factor c_f are calculated using the following equation:

$$\tau_w = c_f(\rho^* V_s^2/2) \qquad (6)$$

$$c_f = 0.664/\sqrt{Re^*} = 0.664/\sqrt{\rho^* V_e x/\mu^*} \qquad (7)$$

The Stanton number appearing in Equation 2 is obtained using the following relationship:

$$C_H = (c_f/2)(Pr^*)^{-2/3} \qquad (8)$$

The convective heat transfer rate can now be calculated using Equation 1.

Figure 7 shows the Stanton number (C_H) as a function of the Reynolds number calculated using the analytical approach and
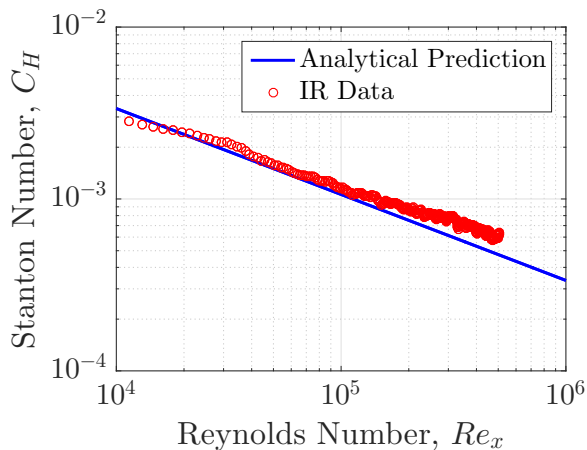
Figure 7: Heat transfer data from analytical method compared to the experimental data for a laminar boundary layer on a flat plate.

is compared with the data derived from the experiment. The data for the Stanton number and Reynolds number were generated from IR image pixels along the center line of the flat plate. From the results in Figure 7, there is a maximum discrepancy of about 15% between the present data and the laminar boundary layer solution. Uncertainty in the material properties of the substrate may contribute to this discrepancy. A more rigorous temperature calibration procedure for the IR camera may also be needed. Further calibration of the IR camera will be conducted using a blackbody source.

Conclusions

An Infra-Red camera has been used to quantify the convective heat transfer on a double swept-wedge configuration. The double swept-wedge configuration was tested in a Ludwieg Tube facility with a nominal Mach number of 5.85 for 200 milliseconds. The IR data was acquired at 100 frames per second (fps) using a Mid Wave Infra Red (MWIR) camera with a spectral bandwidth of 3.6 μm to 4.9 μm. The IR intensity maps are converted to temperature maps using a calibration procedure based on heating up of a copper plate using a hot plate. An average surface heat flux distribution has been generated for the tested configuration using the temperature history recorded by the IR images. The double swept-wedge configuration is subjected to high heat transfer rates at the cowl closure region due to the presence of the corner shock and possible boundary layer separation and reattachment. The heat transfer measurement technique using the IR camera has been compared for a flat plate laminar boundary layer against analytical predictions and differences of around 15% are evident. Substrate material properties uncertainty is a likely contributor, and a more detailed calibration procedure will be undertaken for future work. Nonetheless, it has been shown that this measurement technique can be relied upon to provide a good estimate of the surface heat flux levels for complicated geometric configurations that otherwise would be difficult to instrument. Moreover, this technique provides a global surface measurement for a given geometry compared to discrete measurement techniques such as heat flux gauges.

Acknowledgements

References

[1] Anderson, J.D., Hypersonic and High-Temperature Gas Dynamics, *AIAA Education Series, American Institute of Aeronautics and Astronautics*, **2nd edition**, 2006

[2] Henckels, A. and Maurer, F., Applications of Infra-red Thermography in a Hypersonic Blowdown Wind Tunnel, *International Congress on instrumentation in Aerospace Simulation Facilities*, Göttingen, 1989

[3] Benedetto, S. D., Rufolo, G. C., Marini, M., and Trifoni, E. , European Experimental Reentry Testbed Winglet: From In-Flight Characterization to SCIROCCO Test. *AIAA Journal*, **Vol. 50, No. 10**, 2012

[4] Smart, M.K., Design of Three-Dimensional Hypersonic Inlets with Rectangular-to- Elliptical Shape Transition, *Journal of Propulsion and Power*, **Vol. 15, No. 3**, 1999

[5] Barth, J.E., Wheatley, V., & Smart, M.K., Hypersonic Turbulent Boundary-Layer Fuel Injection and Combustion: Skin-Friction Reduction Mechanisms, *AIAA Journal*, **Vol. 51 No. 9**, 2013

[6] Buttsworth, D. R., Ludwieg Tunnel Facility with Free Piston Compression Heating for Supersonic and Hypersonic Testing, *Ninth Australian Space Science Conference, National Space Society of Australia Ltd.*, Sydney, Australia, Sept. 2009

[7] Widodo, A., and Buttsworth, D. R., Stagnation Temperature in a Cold Hypersonic Flow Produced in a Light Free Piston Compression Facility, *Experiments in Fluids*, **Vol. 54, No. 4**, March 2013

[8] Oldfield, M.,L., Impulse Response Processing of Transient Heat Transfer Gauge Signals, *Journal of Turbomachinery*, **Vol. 130, No. 2**, 2008

[9] Eckert, E.R.G., Engineering Relations for Friction and Heat Transfer to Surfaces in High Velocity Flow, *Journal of the Aeronautical Sciences*, **Vol. 22, No. 8**, 1955